THE JOURNAL OF BIOLOGICAL CHEMISTRY VOL. 285, NO. 23, pp. 17507–17513, June 4, 2010
© 2010 by The American Society for Biochemistry and Molecular Biology, Inc. Printed in the U.S.A.

GDP-Tubulin Incorporation into Growing Microtubules Modulates Polymer Stability*[S]

Received for publication, December 28, 2009, and in revised form, April 1, 2010 Published, JBC Papers in Press, April 6, 2010, DOI 10.1074/jbc.M109.099515

Odile Valiron[‡1], Isabelle Arnal[‡§], Nicolas Caudron[‡], and Didier Job[‡]

From the [‡]Institut National de la Santé et de la Recherche Médicale Unité 836, Institut des Neurosciences de Grenoble, Université Joseph Fourier, 38042 Grenoble, Cedex 9 and the [§]Interactions Cellulaires et Moléculaires, Centre National de la Recherche Scientifique, Unité Mixte de Recherche 6026, Institut Fédératif de Recherche 140, Génétique Fonctionnelle Agronomie et Santé, Université de Rennes 1, Campus de Beaulieu, 263, Avenue du Général Leclerc, 35042 Rennes, France

Microtubule growth proceeds through the endwise addition of nucleotide-bound tubulin dimers. The microtubule wall is composed of GDP-tubulin subunits, which are thought to come exclusively from the incorporation of GTP-tubulin complexes at microtubule ends followed by GTP hydrolysis within the polymer. The possibility of a direct GDP-tubulin incorporation into growing polymers is regarded as hardly compatible with recent structural data. Here, we have examined GTP-tubulin and GDP-tubulin incorporation into polymerizing microtubules using a minimal assembly system comprised of nucleotide-bound tubulin dimers, in the absence of free nucleotide. We find that GDP-tubulin complexes can efficiently co-polymerize with GTP-tubulin complexes during microtubule assembly. GDP-tubulin incorporation into microtubules occurs with similar efficiency during bulk microtubule assembly as during microtubule growth from seeds or centrosomes. Microtubules formed from GTP-tubulin/GDP-tubulin mixtures display altered microtubule dynamics, in particular a decreased shrinkage rate, apparently due to intrinsic modifications of the polymer disassembly properties. Thus, although microtubules polymerized from GTP-tubulin/GDP-tubulin mixtures or from homogeneous GTP-tubulin solutions are both composed of GDP-tubulin subunits, they have different dynamic properties, and this may reveal a novel form of microtubule "structural plasticity."

In mammalian cells, microtubules are centrally involved in many vital processes such as cell morphogenesis and motility. Microtubule arrays display substantial variations in their dynamic behavior, depending on the cell cycle or on the cell type, and this dynamic character is crucial to microtubular functions. The building blocks of microtubules are $\alpha\beta$-tubulin heterodimers. Tubulin subunits associate laterally and longitudinally into growing microtubules (1, 2) in the form of either tubulin dimers or oligomers (3–5). Microtubules shorten through tubulin oligomer loss (6). It is currently assumed that the GDP-tubulin subunits (GDP-tub)[2] that build up the microtubule wall originate from the incorporation of GTP-tubulin complexes (GTP-tub) followed by GTP hydrolysis in the polymer wall (7).

Microtubule growth displays spontaneous transitions between growing and shrinking states, known as dynamic instability (8). Microtubule length variations are currently viewed as principally governed by the behavior of the microtubule ends (9). It has long been assumed that GTP hydrolysis at the extremity of microtubules determined tubulin addition and loss (10). Recent studies show that for a given nucleotide-bound state of the tubulin dimers, microtubule length fluctuations are also dependent on structural events occurring at polymer ends. For example, microtubule tip-binding proteins such as EB1 can regulate dynamics, and tip structure of microtubules assembled from purified tubulin (11) and structural differences between microtubule tips have been shown in studies on kinetochore-microtubule interactions (12). This reveals that microtubule ends can also experience "structural plasticity" (13). Although the switch-like behavior of ends is essential for dynamic instability, microtubules could also exhibit structural plasticity along their length (13, 14). Such plasticity could imply that the tubulin subunits constituting the microtubule wall exist in several structural and/or biochemical states that may influence microtubule dynamic properties (13, 14).

Although the dominant view is currently that microtubule growth proceeds exclusively from the incorporation of GTP-tub, there are scattered reports of direct GDP-tub incorporation into growing polymers (15, 16). However, other studies indicate that GDP-tub does not significantly participate in elongation (17–19). Additionally, recent structural studies have revealed differences between GTP-tub and GDP-tub intradimer and interdimer interactions. This led to the suggestion that GDP-tub could not be directly incorporated in microtubules under any conditions (7). Here, we have re-examined the possibility of a direct GDP-tub incorporation into growing microtubules, using a minimal tubulin assembly system composed of nucleotide-bound tubulin dimers, in the absence of

* This work was supported by grants from La Ligue Nationale Contre le Cancer (to O. V. and D. J.) and Agence Nationale de la Recherce Grant ANR-07-PCVI-0012 (to I. A.).

[S] The on-line version of this article (available at http://www.jbc.org) contains supplemental Results and Figs. S1–S4.

[1] To whom correspondence should be addressed: Grenoble Institut des Neurosciences, Bâtiment Edmond J. Safra, Université Joseph Fourier, Site Santé La Tronche, BP 170, 38042 Grenoble, Cedex 9, France. Tel.: 33-4-56-52-05-37; Fax: 33-4-56-52-06-57; E-mail: odile.valiron@ujf-grenoble.fr.

[2] The abbreviations used are: GDP-tub, GDP-tubulin complex; GTP-tub, GTP-tubulin complex; Detyr-tub, detyrosinated tubulin; Tyr-tub, tyrosinated tubulin; GMPCPP, guanylyl-(α,β)-methylene-diphosphonate; EGS, glycol-bis-succinimidylsuccinate; Mes, 4-morpholineethanesulfonic acid; Pipes, 1,4-piperazinediethanesulfonic acid; GTP-tub/GDP-tub mix, GTP-tub and GDP-tub mixture; EGS-seeds, EGS cross-linked microtubule seeds.

excess free nucleotide (15, 20–22). Within the framework of our study, such a minimal system had substantial advantage over the usual systems in which tubulin assembles in the presence of excess of free GTP. The proportion of GTP-tub and GDP-tub added in solution could be controlled at will without the complication of excess free GTP competing with GDP for the tubulin nucleotide binding site. When GTP-tub assembles above the critical concentration in bulk assembly tests, microtubules undergo a phase of assembly followed by a phase spontaneous disassembly (15, 20–22), which allows monitoring of both assembly and disassembly dynamics. Additionally, in the present study, a similar minimal assembly system proved to be usable for study of individual microtubule dynamics at tubulin concentrations below the critical concentration, using short microtubule seeds or centrosomes to nucleate tubulin assembly. Using such minimal assembly systems, we show that substantial amounts of GDP-tub can be incorporated in growing microtubules during both microtubule bulk assembly and seed- or centrosome-nucleated microtubule assembly. Microtubules assembled from GTP-tub and GDP-tub mixtures (GTP-tub/GDP-tub mix) display altered dynamics. Our results suggest that the GDP-tub constituting the microtubule wall may be in different structural states according to their initial nucleotide-bound state, with resulting variations in intrinsic microtubule disassembly properties. This may reveal a novel form of microtubule structural plasticity.

EXPERIMENTAL PROCEDURES

Tubulin Preparation—Tubulin was purified from fresh bovine brain as described previously (23). To prepare GTP-tub or [^{3}H]GTP-tub, pure tubulin was incubated in PEM buffer (100 mM Pipes (pH 6.7), 1 mM EGTA, 1 mM $MgCl_2$) for 10 min at 4 °C in the presence of either 1 mM GTP (for GTP-tub) or 0.5 mM GTP supplemented with 100 μCi/μM [^{3}H]GTP (for [^{3}H]GTP-tub). Free nucleotides were removed using BioGel P-30 (Bio-Rad) chromatography.

GDP-tub or [^{3}H]GDP-tub was obtained as the cold disassembly product of microtubules initially polymerized from pure tubulin (100 μM) during 20 min at 35 °C in PEM buffer in the presence of 5 mM $MgCl_2$, 30% (v/v) glycerol, and either 1 mM GTP or 0.5 mM GTP with 100 μCi/μM [^{3}H]GTP. After tubulin assembly, microtubules were centrifuged at 179,000 g during 1 h at 35 °C on a cushion containing PEM buffer with 60% glycerol. The pellet was washed two times with PEM at 35 °C. GDP-tub and [^{3}H]GDP-tub were obtained after dilution in PEM buffer at 4 °C of pellets of microtubules assembled from either GTP alone or GTP and [^{3}H]GTP mixtures, respectively.

Tyrosinated tubulin (Tyr-tub) was prepared according to Paturle *et al.* (24). Briefly, tubulin was equilibrated in MEM buffer (100 mM Mes, 1 mM EGTA, 1 mM $MgCl_2$) through BioGel P-30 chromatography. Then tubulin (44 μM final concentration) was incubated in MEM buffer containing ATP (5 mM), dithiothreitol (5 mM), $MgCl_2$ (25 mM), tyrosine (0.5 mM), KCl (100 mM), and tubulin tyrosine ligase (50 μl/ml) at 30 °C for 30 min. The sample was cooled down on ice and centrifuged at 200,000 × *g* at 4 °C for 10 min to remove tubulin aggregates. The supernatant containing Tyr-tub was subjected to gel filtration in BioGel P-30 equilibrated in PEM buffer.

To prepare detyrosinated tubulin (Detyr-tub), purified tubulin (50 μM) was incubated with carboxypeptidase A (2 μg/ml) during 15 min at 30 °C. The reaction was stopped with the addition of 20 mM dithiothreitol. Aggregates were removed by centrifugation (200,000 × *g*, 10 min, 4 °C). Dithiothreitol was removed by gel filtration through BioGel P-30 chromatography.

Microtubule Assembly Conditions—GTP-tub, GTP-tub/GDP-tub mix, or radioactive tubulin mixtures (either [^{3}H]GTP-tub alone or [^{3}H]GTP-tub/GDP-tub mix or GTP-tub/[^{3}H]GDP-tub mix) were aliquoted (20 μl) at 4 °C in tubes. Tubulin assembly was initiated by immersing tubes in a water bath at 35 °C. At selected time points, the reactions were stopped. Stop procedures and further processing of the samples were adapted to the parameter to be measured, as described below (under "Filter Assay") and in the supplemental Results (under "Quantitative Analysis of Microtubule Nucleation and Mean Length Of Microtubules Assembled from GTP-tub/GDP-tub Mixtures" and "Microtubule Sedimentation Assay"). All measurements were done in triplicate.

Filter Assay—To estimate polymeric radioactive tubulin concentration at selected time points, we used a previously developed filter assay (25), with minor modifications. Briefly, either [^{3}H]GTP-tub alone or [^{3}H]GTP-tub/GDP-tub mix or GTP-tub/[^{3}H]GDP-tub mix were prepared at 4 °C, aliquoted, and assembled as above. Tubulin assembly was stopped by adding to samples 1 ml of 100 mM Mes (pH 6.7) containing 1 mM EGTA, 1 mM $MgCl_2$, 0.75% glutaraldehyde, and 50% (w/v) sucrose (25). GF/F glass fiber filters (one filter per time point aliquot) were placed in a vacuum filtration device and washed with 4 ml of PEM buffer containing 25% glycerol (buffer PEM-G). Microtubule suspensions were applied to filters under negative pressure. At this step, ^{3}H-labeled cross-linked microtubules were trapped on the filters, and the bulk of unassembled subunits passed through the filters. Then the filters were washed three times with 4 ml of PEM-G buffer. To extract ^{3}H radioactivity from the filters, they were incubated under shaking during 30 min with 2 ml of ethanol in vials (one vial per filter). Then liquid scintillation mixture was added (10 ml/vial), and radioactivity was counted. Polymerized [^{3}H]tubulin concentrations were estimated from the radioactivity measured on the filters and from the specific activity of [^{3}H]tubulin obtained during tubulin preparation. The [^{3}H]tubulin specific activity (cpm/μmol of tubulin) was calculated as the ratio of the number of cpm contained in an aliquot of the starting tubulin solution over the amount of tubulin contained in the same aliquot.

Preparation of EGS Cross-linked Microtubule Seeds (EGS-Seeds)—Covalently cross-linked microtubule seeds were prepared using ethylene glycol-bis-succinimidylsuccinate (EGS) (26). Tubulin (100 μM) in a total volume of 200 μl was assembled for 15 min at 35 °C in 80 mM Pipes (pH 6.7), 1 mM EGTA, 50% (v/v) glycerol, 5 mM $MgCl_2$, and 1 mM GTP. Microtubules were cross-linked by incubation for 15 min at 35 °C after the addition of 3.4 mM final concentration of EGS. To quench the EGS in excess, the mixture was diluted into 1.8 ml of a buffer containing 80 mM Pipes (pH 6.7), 1 mM EGTA, 50% sucrose, 10 mM glutamate, and 1 mM $MgCl_2$ and incubated for 1 h at room temperature. The solution was then centrifuged at 200,000 × *g*

for 1 h at room temperature. The pellet containing cross-linked microtubules (EGS-seeds) was resuspended in 80 μl of PEM buffer.

Microtubule Immunostaining—In microtubule self-assembly conditions (overcritical GTP-tub concentration), after stopping the assembly reaction, microtubules were diluted in PEM buffer supplemented with 10% glycerol. They were then centrifuged on coverslips at 77,000 × *g* during 30 min at room temperature and fixed with methanol for 6 min at −20 °C. Coverslips were processed for indirect immunofluorescence analysis as described previously (27) using primary anti-Detyr-tub antibody (28) and primary anti-Tyr-tub antibody (clone YL1/2 (29)). At subcritical GTP-tub concentration, microtubules were nucleated on centrosomes as described (30) and immunolabeled as above.

Video Microscopy and Data Analysis—Video microscopy and analysis were performed as described previously (31). Briefly, samples were prepared in perfusion chambers. Purified centrosomes were first perfused into the chamber on ice. Samples (60 μl) containing either GTP-tub or GTP-tub/GDP-tub mix were then perfused in the chamber, and microtubule assembly was observed at 37 °C under an Olympus BX51 microscope equipped with differential interference contrast prisms and a camera (Sony, XC-ST70/CE). Images were recorded every 2 s, and microtubule dynamics measurements and data analysis were performed using the NIH Image and KaleidaGraph software programs. For growth and shrinkage rates, standard deviations were calculated as S.E., assuming a normal data distribution. For catastrophe frequencies, standard deviations were calculated as catastrophe frequency/($\sqrt{n}$), where *n* is the number of events counted, assuming a Poisson distribution (32).

RESULTS

GDP-tub Incorporates in Self-assembled Microtubules and Modulates Their Assembly-Disassembly Properties—We tested the incorporation of GTP-tub or GDP-tub into growing microtubules in a chemically simple system (15, 20–22) in which microtubules were assembled from solutions containing GTP-tub/GDP-tub mix in the absence of free nucleotide. Starting mixtures contained either [^{3}H]GTP-tub and unlabeled GDP-tub or unlabeled GTP-tub and [^{3}H]GDP-tub. We verified (supplemental Results, Fig. S1) that our tubulin preparations were devoid of detectable amounts of nucleoside-diphosphate kinase activity, which could induce conversion of free GDP-tub to free GTP-tub during our experiments (33). The incorporation of either GTP-tub or GDP-tub in microtubules assembled from GTP-tub/GDP-tub mix could then be selectively monitored by counting the ^{3}H-nucleotide radioactivity associated to microtubules trapped on filters (see "Experimental Procedures") (22).

In the absence of GDP-tub, GTP-tub assembly follows a bell-shaped curve, with a phase of microtubule assembly followed by a phase of microtubule disassembly (Fig. 1*A*), as described before (22). In our experiments, in agreement with previous reports (7, 19), GDP-tub alone was unable to polymerize (not shown). The addition of GDP-tub to GTP-tub did not detectably modify the maximum of GTP-tub incorporation into

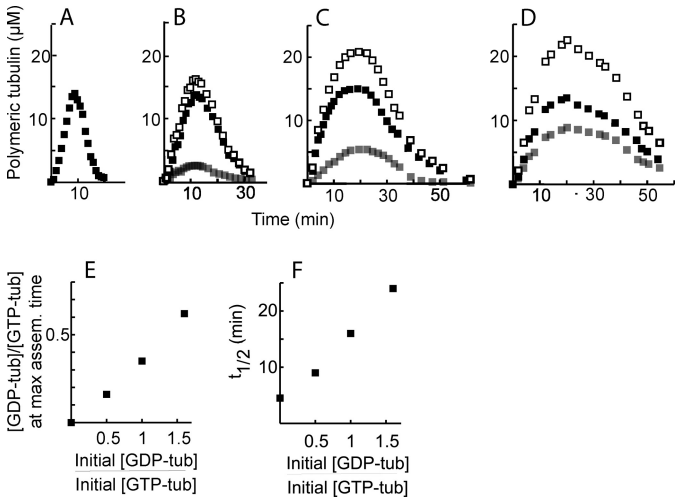

FIGURE 1. **GDP-tub incorporation in spontaneous nucleated microtubules.** *A–D*, GTP-tub (75 μM) was assembled in the absence (*A*) or in the presence of GDP-tub (37.5 μM (*B*), 75 μM (*C*), or 120 μM (*D*)). Either GTP-tub or GDP-tub was ^{3}H-labeled, and ^{3}H incorporation in microtubules was determined to measure GTP-tub (■) or GDP-tub (▨) incorporation. Total polymeric tubulin (□) was calculated by the summation of the GDP-tub and GTP-tub curves. *E*, plot of (polymeric GDP-tub concentration/polymeric GTP-tub concentration) ratios at maximum assembly time (*max assem. time*) *versus* (initial GDP-tub concentration/initial GTP-tub concentration) ratio. *F*, microtubule half-disassembly times $t_{1/2}$ *versus* (initial GDP-tub concentration/initial GTP-tub concentration) ratio. $t_{1/2}$ values were determined from the plots shown in *panels A–D*.

microtubules (Fig. 1, *A–D* (■)). Interestingly, when [^{3}H]GDP-tub was mixed with GTP-tub in starting suspension, [^{3}H]GDP-tub was incorporated in assembling microtubules (Fig. 1, *B–D* (▨)). GDP-tub incorporation occurred in amounts proportional to the initial GDP-tub/GTP-tub ratio (Fig. 1*E*). As a result of the incorporation of GDP-tub, the total tubulin assembly level increased at rising initial GDP-tub concentrations (Fig. 1, *A–D* (□)). The assembly phase was prolonged, whereas in a quantitative analysis, initial microtubule nucleation and elongation seemed little affected (supplemental Results, supplemental Fig. S2). The disassembly phase was conspicuously prolonged at increasing GDP-tub concentrations to such an extent that instead of exhibiting a characteristic symmetry bell-shaped aspect (Fig. 1*A*), the tubulin assembly-disassembly curve became right-skewed (Fig. 1*D*). When compared with the control, the bulk microtubule half-disassembly time increased 5-fold at a 1.5/1 initial GDP-tub/GTP-tub ratio (Fig. 1*F*).

In a series of control experiments, tubulin assembly was monitored using either turbidity measurements (supplemental Results, Fig. S3) or microtubule sedimentation assays (supplemental Results, Fig. S4). In turbidity assays, GDP-tub alone was unable to polymerize, whereas the addition of excess free GTP produced the expected sustained microtubule assembly (supplemental Results, supplemental Fig. S1*A*). The assembly of GTP-tub/GDP-tub mix yielded assembly plots similar to those observed in the same conditions using filter assays (Fig. 1, *A–D*), which was also the case of assembly plots derived from microtubule sedimentation assays (supplemental Results, Fig. S4).

These results provide compelling evidence that GDP-tub can be directly co-incorporated into growing microtubules, together with GTP-tub. Additionally, our results suggest that

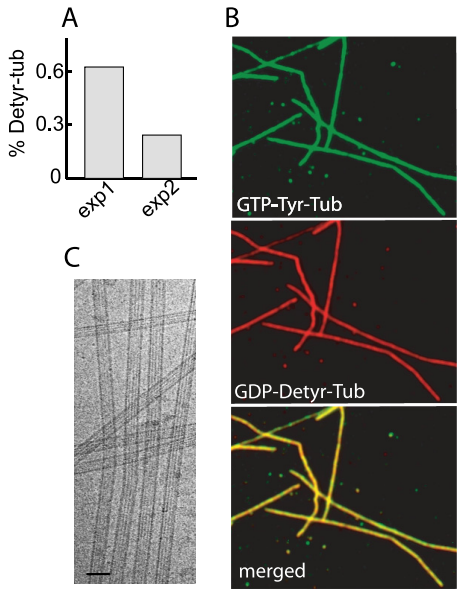

FIGURE 2. **Visualization of GDP-tub incorporation into microtubules.** *A*, microtubules were assembled from GTP-Detyr-tub (70 μM) and GDP-Tyr-tub (50 μM) (*exp1*) or from GTP-Tyr-tub (70 μM) and GDP-Detyr-tub (50 μM) (*exp2*). Microtubule composition at the time of maximum assembly was analyzed on immunoblots (supplemental Results). The histogram shows the percentage of Detyr-tub in microtubules. *B*, light microscopy examination of microtubules assembled from GTP-Tyr-tub and GDP-Detyr-tub during 10 min at 35 °C in PEM buffer. The *bottom panel* shows superposition of both images. *C*, cryo-electron microscopy images of the microtubules assembled from GTP-tub (75 μM) and GDP-tub (120 μM).

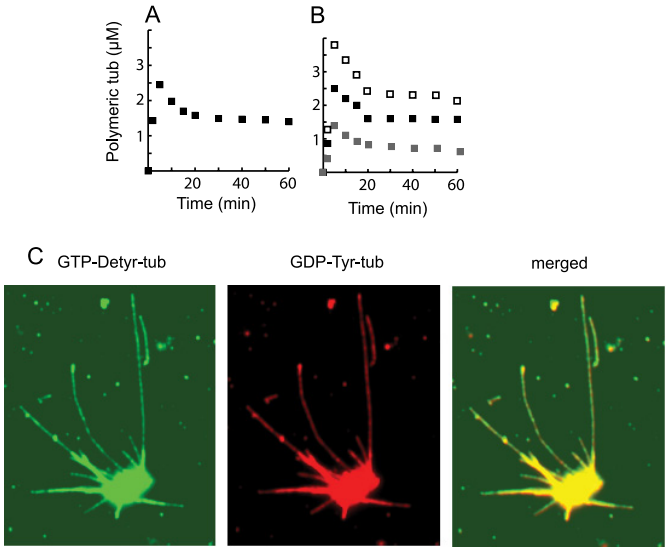

FIGURE 3. **GDP-tub incorporation in microtubules nucleated on seeds or on centrosomes.** *A* and *B*, microtubules were assembled from GTP-tub (25 μM) in the presence of microtubule seeds without (*A*) or with GDP-tub (12.5 μM) (*B*). Either GTP-tub or GDP-tub was radiolabeled with ^{3}H, and ^{3}H incorporation in microtubules was determined to measure GTP-tub (■) or GDP-tub (▨) incorporation. Total polymeric tubulin (□) was calculated by the summation of the GDP-tub and GTP-tub curves. *C*, light microscopy examination of microtubules assembled from centrosomes in the presence of GTP-Detyr-tub (25 μM) and GDP-Tyr-tub (8.3 μM) during 10 min at 35 °C in PEM buffer. Both tubulin isotypes were labeled with specific antibodies.

GDP-tub incorporation in microtubules could impair microtubule disassembly.

GDP-tub Co-assembly Occurs along the Whole Polymer Length but Does Not Induce Detectable Changes in the Microtubule Lattice Organization—To directly visualize GDP-tub incorporation into microtubules, we used GDP-tub or GTP-tub made of different tubulin tyrosination variants. Previous work has shown that tubulin tyrosination variants such as Tyr-tub and Detyr-tub have distinct immunoreactivity properties (34) but have indistinguishable *in vitro* assembly properties (24). To test the reliability of tubulin variants as reporters of the tubulin-bound nucleotide state, GDP-Detyr-tub was mixed with GTP-Tyr-tub or, in symmetric experiments, GTP-Detyr-tub was mixed with GDP-Tyr-tub. Tubulin mixtures were assembled at 35 °C, and sedimented microtubules were assayed for their tubulin composition. The proportion of Detyr-tub or Tyr-tub incorporated in microtubules was a function of the initial Detyr-tub- or Tyr-tub-bound nucleotide state and was in good agreement with the ratio of GTP-tub/GDP-tub incorporation estimated from radioactive measurements (Fig. 2*A* and supplemental Results). Thus, over the time course of our experiments, the association of each tubulin variant with its bound nucleotide was stable enough to allow qualitative visualization of GDP-tub incorporation in growing microtubules. Microtubules assembled from Tyr-GTP-tub/Detyr-GDP-tub mix were then sedimented and double-stained with Tyr-tub and Detyr-tub antibodies. Immunofluorescence analysis showed that polymers were uniformly and homogeneously stained by both antibodies (Fig. 2*B*). These results indicate that GDP-tub is incorporated in growing microtubules during the whole assembly process.

We then used cryo-electron microscopy to examine the structure of microtubules assembled either from GTP-tub alone or from GTP-tub/GDP-tub mix (Fig. 2*C*). Based on the moiré pattern observed on microtubule images, we determined the microtubule protofilament number and the frequency of lattice defects as described previously (35, 36). We also assessed the aspect of microtubule ends in polymerizing and depolymerizing conditions, and we analyzed the disassembly products of polymers exposed to high calcium concentrations (37, 38). We found no significant difference between GTP-tub or GTP-tub/GDP-tub polymers (not shown). Thus, incorporation of GDP-tub into microtubules did not induce any obvious changes in the polymer structure.

GDP-tub Incorporated into Microtubules Nucleated from Seed or Centrosomes—The experiments shown above were performed at high initial tubulin concentrations, compatible with efficient spontaneous microtubule nucleation. We investigated whether GDP-tub could also be incorporated in growing microtubules at subcritical tubulin concentrations, in seed- or centrosome-nucleated tubulin assembly conditions. In our experiments, the critical concentration was 30 μM. The incorporation of GDP-tub in microtubules elongating from EGS-seeded microtubules was monitored using filter assays as described above (Fig. 1, *B–D*). Fig. 3, *A* and *B*, show that microtubules assembled from tubulin solutions containing GDP-tub and GTP-tub in a 0.5/1 proportion incorporated nearly one molecule of GDP-tub for two molecules of GTP-tub. We then tested whether GDP-tub incorporation occurred in microtubules nucleated on centrosomes by using immunofluorescence microscopy and tubulin variants as markers of GDP-tub and GTP-tub incorporation. Again, results showed apparently homogeneous qualitative incorporation of GDP-tub during

A

GTP-tub (μM) GDP-tub (μM)	25 0	25 3.8	25 7.6	25 8.3	25 12.5
Growth rate (μm/min)	2.30 (0.81) n=379	2.39 (0.78) n=228	2.03 (0.70) n=174	1.89 (0.81) n=245	1.46 (0.69) n=210
Shrinkage rate (μm/min)	32.04 (14.33) n=80	37.33 (15.34) n=38	25.09 (16.46) n=55	23.62 (13.63) n=68	16.88 (12.58) n=63
Catastrophe freq (event/min)	0.17 (0.034) n=25	0.13 (0.039) n=11	0.17 (0.049) n=12	0.21 (0.048) n=19	0.30 (0.064) n=22
Time of recording (min)	149	85	71	94	74

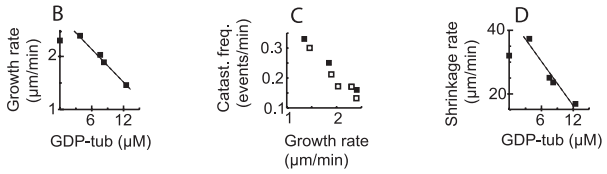

FIGURE 4. **Microtubules grown from centrosomes: effects of GDP-tub on microtubular dynamics.** *A*, dynamic parameters of microtubules polymerized from centrosomes and GTP-tub (25 μM) in the presence of increasing GDP-tub concentrations. Standard deviations are represented in *parentheses*. *n*, number of events. *B*, microtubule growth rate *versus* GDP-tub concentration. *C*, catastrophe frequency (*Catast. freq.*) *versus* growth rate of microtubules assembled with increasing concentrations (18, 22, 25 and 28 μM) of GTP-tub (*black squares*) or with 25 μM GTP-tub in the presence of increasing GDP-tub concentrations (*empty squares*). *D*, microtubule shrinkage rate *versus* GDP-tub concentration.

assembly (Fig. 3*C*). These results indicate robust and direct incorporation of GDP-tub into seed- or centrosome-nucleated microtubules at subcritical tubulin concentrations.

Dynamic Behavior of Centrosome-nucleated Microtubules Assembled in the Presence of GDP-tub—Microtubules nucleated on centrosomes were visualized by standard video differential interference contrast microscopy for direct tests of GDP-tub effects on individual polymer dynamics. Centrosomes were preadsorbed on the surface of a perfusion chamber. Samples containing GTP-tub (25 μM) without or with increasing GDP-tub concentrations (from 5 to 25 μM) were then injected into the chamber and observed under the microscope at 37 °C. In these conditions, the average microtubule growth rate was unaffected by the addition of up to 3.8 μM GDP-tub. In the 3.8–12.5 μM GDP-tub concentration range, the average growth rate decreased linearly with the GDP-tub concentration (Fig. 4, *A* and *B*). GDP-tub concentrations above 12.5 μM inhibited microtubule nucleation on centrosomes.

The catastrophe frequency increased when microtubules were assembled in the presence of GDP-tub concentration from 7.6 μM and above (Fig. 4*A*). It has been shown that at subcritical GTP-tub concentration, microtubule catastrophe rates increase with decreased elongation rates (32, 39). Here, the elongation rate was lower in the presence of GDP-tub when compared with control. To know whether the decrease in elongation rate accounted for increased catastrophe rate, we compared catastrophe frequencies *versus* growth rate in the absence (Fig. 4*C*, *black symbols*) and in the presence (Fig. 4*C*, *empty symbols*) of added GDP-tub. Plot analysis showed similar catastrophe rates at equal elongation rates, regardless of the presence or absence of added GDP-tub at the onset of assembly.

TABLE 1

Microtubule shrinkage in different conditions

Microtubules were assembled from GTP-tub (65 μM) at room temperature. Microtubule shrinkage rates were measured either during spontaneous catastrophes (control) or after chamber perfusion with PEM buffer alone or PEM buffer containing 65 μM GDP-tub as indicated. Standard deviations are represented in parentheses. *n*, number of events.

	Experimental conditions		
	Perfusion with PEM	Perfusion with GDP-tub (65 μM)	Control GTP-tub (65 μM)
Shrinkage rate (μm/min)	−11.24 (7.04) $n = 200$	−11.70 (5.34) $n = 228$	−16.74 (11.22) $n = 77$

These results indicate that in our experimental conditions, GDP-tub addition increased the catastrophe frequency due to a decrease in the polymer growth rate in the absence of detectable modification of intrinsic microtubule catastrophe properties.

Interestingly, the microtubule shrinkage rate decreased linearly with increasing GDP-tub concentration above 3.8 μM, being ~50% inhibited at a 12.5 μM GDP-tub concentration (Fig. 4*D*). Microtubule shrinkage has been previously demonstrated to be a zero order reaction, depending on the intrinsic structural properties of microtubules, not on the composition of the soluble tubulin pool (8). Accordingly, shrinkage rates were similar when chambers containing microtubules grown from centrosomes were perfused with PEM buffer alone or in the presence of added GDP-tub complexes (Table 1). The shrinkage rate was also in the same range during the spontaneous catastrophes observed in control samples, containing only GTP-tub in the soluble pool (Table 1). We also checked that in the range of GTP concentrations used in our study, the shrinkage rate of microtubules assembled at various GTP-tub concentrations was not significantly correlated with the microtubule growth rates, as shown previously (32).

Collectively, our results indicate that direct GDP-tub incorporation into the microtubule wall occurs in both self-assembled microtubules and seed-nucleated polymers. GDP-tub incorporation apparently induces a decrease of the microtubule growth rate and the microtubule shrinkage rate. The decrease of the shrinkage rate most probably results from a modification of the intrinsic stability properties of microtubules.

DISCUSSION

In this study, we show substantial GDP-tub incorporation into polymerizing microtubules with resulting impaired microtubule dynamic parameters. The main novelty of our study is the use of a simple system containing only GTP-tub and GDP-tub without any free nucleotide, allowing direct measurements and visualization of the incorporation of both GTP-tub and GDP-tub.

The possibility of a direct incorporation of GDP-tub into polymerizing microtubules has been the subject of controversy. Based on turbidimetry measurements, previous studies have suggested GDP-tub incorporation in the microtubule wall (15, 16), which has been questioned in subsequent work (17–19). Additionally, direct GDP-tub incorporation seemed precluded according to recent structural studies indicating that the shape of GDP-tub does not fit the microtubule lattice (7). Our data show a different picture, demonstrating that robust and sub-

stantial direct GDP-tub incorporation into growing microtubules can be achieved. However, GDP-tub incorporation in microtubules occurs only if GTP-tub is also present at a concentration sufficient to support microtubule assembly, indicating obligatory co-incorporation of GTP-tub with GDP-tub. It has been suggested that microtubule assembly can involve the incorporation of tubulin oligomers (3). Maybe GDP-tub can be incorporated by "hitchhiking" polymerizing GTP-tub oligomers, although other models are possible. Such a co-incorporation of GDP-tub with GTP-tub fits with recent studies indicating that GTP-tub and GDP-tub may be similarly bent and that subunits straighten only after their incorporation into microtubules (40, 41).

Our data indicate that neither initial microtubule nucleation nor initial microtubule elongation was sizably affected by GDP-tubulin incorporation during microtubule assembly in our bulk microtubule assembly conditions. According to previous work (22), at the high tubulin concentrations used in bulk assembly conditions, the rate of microtubule elongation is limited during most of the assembly phase by intrinsic structural factors such as the speed of tube closure (22). In this view, our data could indicate that tube closure is not impaired by co-incorporation of GDP-tub together with GTP-tub. In apparent contrast, in our study, the growth rate of centrosome-nucleated microtubules decreased at increasing GDP-tub concentrations. However, at subcritical tubulin concentrations, the availability of free tubulin dimers becomes rate-limiting for microtubule growth (32). Our data would then indicate that GDP-tubulin behaves as a competitive inhibitor of GTP-tub when the tubulin concentration becomes rate-limiting.

In the present study, microtubules assembled from GDP-tub/GTP-tub mix displayed impaired disassembly behavior, involving a decrease of the individual polymer shrinkage rate. Previous works have established that hydrolysis of the tubulin-bound nucleotide within the microtubule wall is required for subsequent microtubule disassembly (42, 43). Thus, microtubule disassembly is dramatically impaired when microtubules were assembled in the presence of a slowly hydrolyzable analog of GTP, GMPCPP (42). Obviously, in our experiments, the incorporation of GDP-tub in the polymer wall is not followed by hydrolysis of the bound nucleotide. GDP may thus function as a natural non-hydrolyzable analog of GTP, with resulting impairment of the disassembly properties of microtubules assembled in the presence of GDP-tub.

Whether microtubules are assembled from GTP-tub alone or from GTP-tub/GDP-tub mix, they are ultimately composed of GDP-tub. However, microtubules have different dynamic properties according to the composition of the starting tubulin solution. Such dynamic differences uncoupled to the bound nucleotide state in the microtubule wall provide a striking illustration of the recently proposed concept of microtubule structural plasticity (13).

Microtubules assembled with GMPCPP show detectable modifications in their lattice organization (44) and in the structure of their oligomeric breakdown products (38). We have not detected such modifications in polymers assembled in the presence of GDP-tub. Maybe, in our conditions, lattice modifications are blurred by the mixed incorporation of GTP- and GDP-tub when compared with a homogeneous incorporation of GMPCPP-tubulin complexes in previous work. Alternatively, structural alterations in polymers assembled with GDP-tub may be truly undetectable at the level of electron microscopy resolution.

The fundamental discovery that GTP hydrolysis in the microtubule wall is required for microtubule disassembly (44), not for microtubule assembly as assumed previously, has been a substantial surprise for scientists in the microtubule field. This discovery indicated a strong link between GTP hydrolysis and microtubule stability, a remarkable microtubule feature that cells could use for microtubule regulations. However, exchanging GTP for a slowly hydrolyzable analog is the only known way to modulate the bound nucleotide hydrolysis in the microtubule wall during tubulin assembly, and the existence of a naturally occurring non-hydrolyzable analog of GTP may look like a remote possibility. Our data indicate that GDP may represent such an analog, and a regulation of microtubule disassembly through GDP-tub incorporation in cellular microtubules is an attractive possibility. In the absence of a structural signature allowing visual identification of polymers assembled with GDP-tub, tests of such a possibility may rely on the characterization and manipulation of putative regulatory systems that could modulate the GDP-tub/GTP-tub ratio at the end of cellular microtubules.

Acknowledgments—We thank Dr. Annie Andrieux and Dr. Christian Delphin for critical reading of the manuscript.

REFERENCES

1. Desai, A., and Mitchison, T. J. (1997) *Annu. Rev. Cell Dev. Biol.* **13,** 83–117
2. Valiron, O., Caudron, N., and Job, D. (2001) *Cell Mol. Life Sci.* **58,** 2069–2084
3. Kerssemakers, J. W., Munteanu, E. L., Laan, L., Noetzel, T. L., Janson, M. E., and Dogterom, M. (2006) *Nature* **442,** 709–712
4. Mozziconacci, J., Sandblad, L., Wachsmuth, M., Brunner, D., and Karsenti, E. (2008) *PLos ONE* **3,** e3821
5. Wu, Z., Wang, H. W., Mu, W., Ouyang, Z., Nogales, E., and Xing, J. (2009) *PLoS ONE* **4,** e7291
6. Schek, H. T., 3rd, Gardner, M. K., Cheng, J., Odde, D. J., and Hunt, A. J. (2007) *Curr. Biol.* **17,** 1445–1455
7. Wang, H. W., and Nogales, E. (2005) *Nature* **435,** 911–915
8. Mitchison, T., and Kirschner, M. (1984) *Nature* **312,** 237–242
9. Howard, J., and Hyman, A. A. (2009) *Nat. Rev. Mol. Cell Biol.* **10,** 569–574
10. Carlier, M. F. (1989) *Int. Rev. Cytol.* **115,** 139–170
11. Vitre, B., Coquelle, F. M., Heichette, C., Garnier, C., Chrétien, D., and Arnal, I. (2008) *Nat Cell Biol.* **10,** 415–421
12. McIntosh, J. R., Grishchuk, E. L., Morphew, M. K., Efremov, A. K., Zhudenkov, K., Volkov, V. A., Cheeseman, I. M., Desai, A., Mastronarde, D. N., and Ataullakhanov, F. I. (2008) *Cell* **135,** 322–333
13. Kueh, H. Y., and Mitchison, T. J. (2009) *Science* **325,** 960–963
14. Dimitrov, A., Quesnoit, M., Moutel, S., Cantaloube, I., Poüs, C., and Perez, F. (2008) *Science* **322,** 1353–1356
15. Carlier, M. F., and Pantaloni, D. (1978) *Biochemistry* **17,** 1908–1915
16. Hamel, E., Batra, J. K., and Lin, C. M. (1986) *Biochemistry* **25,** 7054–7062
17. Jameson, L., and Caplow, M. (1980) *J. Biol. Chem.* **255,** 2284–2292
18. Zackroff, R. V., Weisenberg, R. C., and Deery, W. J. (1980) *J. Mol. Biol.* **139,** 641–659
19. Bayley, P. M., Butler, F. M., and Manser, E. J. (1986) *FEBS Lett.* **205,** 230–234
20. Carlier, M. F., Didry, D., and Pantaloni, D. (1997) *Biophys. J.* **73,** 418–427
21. O'Brien, E. T., and Erickson, H. P. (1989) *Biochemistry* **28,** 1413–1422

22. Caudron, N., Valiron, O., Usson, Y., Valiron, P., and Job, D. (2000) *J. Mol. Biol.* **297,** 211–220
23. Paturle-Lafanechère, L., Eddé, B., Denoulet, P., Van Dorsselaer, A., Mazarguil, H., Le Caer, J. P., Wehland, J., and Job, D. (1991) *Biochemistry* **30,** 10523–10528
24. Paturle, L., Wehland, J., Margolis, R. L., and Job, D. (1989) *Biochemistry* **28,** 2698–2704
25. Job, D., Pabion, M., and Margolis, R. L. (1985) *J. Cell Biol.* **101,** 1680–1689
26. Fanara, P., Oback, B., Ashman, K., Podtelejnikov, A., and Brandt, R. (1999) *EMBO J.* **18,** 565–577
27. Peris, L., Thery, M., Fauré, J., Saoudi, Y., Lafanechère, L., Chilton, J. K., Gordon-Weeks, P., Galjart, N., Bornens, M., Wordeman, L., Wehland, J., Andrieux, A., and Job, D. (2006) *J. Cell Biol.* **174,** 839–849
28. Paturle-Lafanechère, L., Manier, M., Trigault, N., Pirollet, F., Mazarguil, H., and Job, D. (1994) *J. Cell Sci.* **107,** 1529–1543
29. Wehland, J., and Weber, K. (1987) *J. Cell Sci.* **88,** 185–203
30. Popov, A. V., Pozniakovsky, A., Arnal, I., Antony, C., Ashford, A. J., Kinoshita, K., Tournebize, R., Hyman, A. A., and Karsenti, E. (2001) *EMBO J.* **20,** 397–410
31. Arnal, I., Heichette, C., Diamantopoulos, G. S., and Chrétien, D. 2004. *Curr. Biol.* **14,** 2086–2095
32. Walker, R. A., O'Brien, E. T., Pryer, N. K., Soboeiro, M. F., Voter, W. A., Erickson, H. P., and Salmon, E. D. (1988) *J. Cell Biol.* **107,** 1437–1448
33. Nickerson, J. A., and Wells, W. W. (1978) *Biochem. Biophys Res Comm* **85,** 820–826
34. Gundersen, G. G., Kalnoski, M. H., and Bulinski, J. C. (1984) *Cell* **38,** 779–789
35. Wade, R. H., Chrétien, D., and Job, D. (1990) *J. Mol. Biol.* **212,** 775–786
36. Chrétien, D., Metoz, F., Verde, F., Karsenti, E., and Wade, R. H. (1992) *J. Cell Biol.* **117,** 1031–1040
37. Tran, P. T., Joshi, P., and Salmon, E. D. (1997) *J Struct Biol* **118,** 107–118
38. Müller-Reichert, T., Chrétien, D., Severin, F., and Hyman, A. A. (1998) *Proc. Natl. Acad. Sci. U.S.A.* **95,** 3661–3666
39. Drechsel, D. N., Hyman, A. A., Cobb, M. H., and Kirschner, M. W. (1992) *Mol. Biol. Cell* **3,** 1141–1154
40. Rice, L. M., Montabana, E. A., and Agard, D. A. (2008) *Proc. Natl. Acad. Sci. U.S.A.* **105,** 5378–5383
41. Buey, R. M., Díaz, J. F., and Andreu, J. M. (2006) *Biochemistry* **45,** 5933–5938
42. Hyman, A. A., Salser, S., Drechsel, D. N., Unwin, N., and Mitchison, T. J. (1992) *Mol. Biol. Cell* **3,** 1155–1167
43. Caplow, M., Ruhlen, R. L., and Shanks, J. (1994) *J. Cell Biol.* **127,** 779–788
44. Hyman, A. A., Chrétien, D., Arnal, I., and Wade, R. H. (1995) *J. Cell Biol.* **128,** 117–125